Report to PAC18, 12 GeV Session:

Measuring F_π at Higher Q^2

G.M. Huber, H.P. Blok, D.J. Mack

on behalf of the Exclusive Reactions Working Group

July 6, 2000

As requested by the White Paper Steering Committee, this report will concentrate on the technical feasibility of a F_π measurement at high Q^2, and the interpretability of the extracted result, rather than on the scientific justification for such a measurement. In this document, we present the case that a measurement of F_π using SHMS and 11 GeV beam is not only highly interesting, but also technically feasible.

1 Scientific motivation

The π^+ electric form factor is a topic of fundamental importance to our understanding of hadronic structure. It is well known [1] that the asymptotic behavior is rigorously calculable in perturbative QCD (pQCD), with value

$$F_\pi \rightarrow \frac{8\pi\alpha_s f_\pi^2}{Q^2},$$

where $f_\pi = 133$ MeV is the $\pi^+ \rightarrow \mu^+\nu$ decay constant. This result is in principle exact, and is dependent only on the assumption of quark asymptotic freedom.

The theoretical prediction for F_π at experimentally accessible Q^2 is less certain, as soft scattering contributions, such as gluonic effects, must be explicitly taken into account. After years of theoretical effort, there has been considerable progress in our understanding of the smallest value of Q^2 for which the hard scattering (asymptotic QCD) prediction of the pion form factor will apply. It is generally expected that the asymptotic region is well beyond the capabilities of Jefferson Lab, even after the energy upgrade, probably near $Q^2 = 15$ GeV^2/c^2 (e.g. [2, 3, 4, 5, 6]).

The most interesting question then, as far as Jefferson Laboratory is able to address, is the description of $F_\pi(Q^2)$ in the gap between the "soft" and "hard" regions. This is a difficult and poorly understood region. For example, Jakob and Kroll [4] found that a self consistent treatment of the pQCD contribution to the pion form factor in the few GeV region requires the inclusion of both Sudakov corrections and the transverse momenta of the quarks, leading to an amount which is nonetheless too small with respect to the data, and leaving room for an important role of other processes, such as higher twists. Braun, Khodjamirian, and Maul [7] performed light-cone sum rule calculation up to twist 6, and found that the non-perturbative hard contributions of higher twist strongly cancel the soft components, even at relatively modest Q^2. The models of references [3, 8, 9] obtain good agreement with the experimental data over a broad region of Q^2 by incorporating a confining potential which dominates at low Q^2, and a QCD-based interaction which dominates at high Q^2 that takes the form of a one gluon exchange potential or dynamic chiral symmetry breaking. Finally, Maris and Tandy [10] use the Bethe-Salpeter plus Schwinger-Dyson equations to determine the pion form factor. In this case, the model's parameters are adjusted to reproduce m_π, f_π, and $< \bar{q}q >$ and

then the predicted F_π is found to have reasonable agreement with the existing data. Reliable experimental data are clearly needed to delineate the role of hard versus soft contributions at intermediate Q^2, and so aid the further development of these models.

The situation for the nucleonic form factors is even more complicated. Firstly, their asymptotic behavior is not predicted in such an unequivocal manner. Secondly, the greater number of valence quarks in the nucleon means that the asymptotic regime will be reached at much higher values of Q^2, at least 100 GeV^2/c^2. Finally, the lower power of Q^2 in the pion form factor means that the relevant cross section will be more easily accessible, and less sensitive to experimental uncertainties in Q^2. Because of these reasons, if one believes that it is worthwhile to pursue the measurement of a hadronic form factor where perturbative effects may become apparent, the pion form factor is the obvious first choice.

2 Interpretability and feasability of the experiment

2.1 How to determine F_π

Because of the ongoing F_π measurements in Hall C, as well as the previous work at Cornell and DESY, many of the experimental difficulties in extracting the pion form factor are well understood. There are a number of issues of importance:

1. To perform measurements above $Q^2 = 0.3$ GeV^2/c^2, one must employ electron scattering off the virtual π^+ (of a proton), and relate the resulting measurement to the on-shell electron-pion scattering amplitude. The dependence on F_π enters the cross section via the t-channel diagram (Figure 1), which in Born term models [12] is given as

$$\frac{d\sigma_L}{dt} \sim \frac{-tQ^2}{(t-m_\pi^2)^2} g_{\pi NN}^2(t) F_\pi^2(Q^2).$$

   The virtual nature of the target comes in via the term $g_{\pi NN}(t)$, which can be seen as the probability amplitude to have a virtual π^+ inside the proton at a given t. An additional complication is that the physical region for t in pion electroproduction is negative, while real electron-pion scattering corresponds to $t = m_\pi^2$.

   For W above the resonance region, the t-channel diagram dominates σ_L for small $|t|$ and contributes unequally to the L, T, TT, and LT responses. The competing non-pole production diagrams contribute to σ_L as well, but they are small in forward kinematics (i.e. small $|t|$) and do not have a pole at $t = m_\pi^2$. Therefore, to maximize the contribution of the t-channel diagram, as well as separate it from the others which tend to disguise its effect, it is absolutely necessary to measure at a low $|t|$ in parallel kinematics, and to perform a response function separation.

   The 11 GeV upgrade is essential for these measurements, because it allows a higher W to be accessed, which results in data obtained at a dramatically lower $|t|$ than previously possible. Regge model [13] calculations indicate that there is in fact a range of W for which the contribution of the t-channel diagram is optimized (Figure 2). $-t_{min}$ decreases (i.e. gets closer to the π^+ pole) from left to right on the figure, with value $t = -0.53$ at $W = 2$, $t = -0.14$ at $W = 3$, and $t = -0.05$ at $W = 4$ GeV.

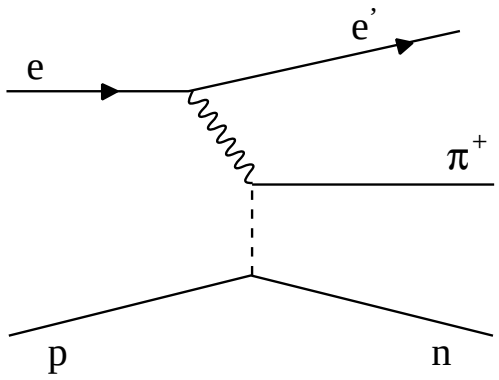

Figure 1: Diagram of the t-channel process.

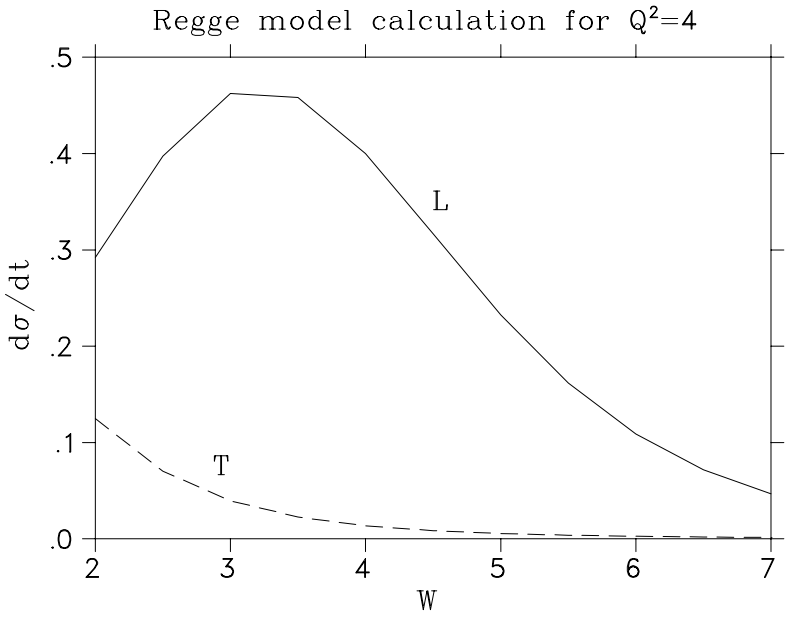

Figure 2: Regge model [13] calculation of the L and T responses in the $p(e, e'\pi^+)n$ reaction at $Q^2 = 4$ GeV^2/c^2, in parallel kinematics.

Nonetheless, $d\sigma_L/dt$ drops dramatically above $W = 3.5$ GeV, and so the optimal value of W for a measurement at $Q^2 = 4$ is near $W = 3.3$ GeV.

The kinematics we propose for this measurement are consistent with these requirements.

2. The presence of isoscalar backgrounds to σ_L can be inferred by measuring the ratio

$$P = \frac{\sigma(p(e, e'\pi^-)p)}{\sigma(p(e, e'\pi^+)n))} = \frac{|A_v - A_s|^2}{|A_v + A_s|^2}.$$

The t-channel diagram is a purely isovector process, and so at small $|t|$, P should be near unity. Isoscalar backgrounds are expected to be suppressed by the L response function extraction. Nonetheless, if they are present to any significant degree, they will result in a dilution of the ratio. **These tests were performed in E93-021, and a preliminary σ_L ratio consistent with unity was obtained over the whole measured range of $|t|$.**

The bottom line is that tests can and must be performed to verify that the longitudinal data are dominated by the t-channel process. This lends confidence in the F_π value extracted from the experiment.

3. It is absolutely essential to use theoretical input for the extraction of F_π.

Frazer [14] originally proposed that F_π be extracted from σ_L via a kinematic extrapolation to the pion pole, and that this be done in an analytical manner, à la Chew-Low. The Born formula, given earlier, is not gauge invariant [13], but should nonetheless give F_π, in principle, when extrapolating to the pole. However, this extrapolation procedure fails to produce a reliable answer, since different polynomial fits, each of which are equally likely in the physical region, differ considerably when continued to $t = m_\pi^2$. Some attempts were made [15] to reduce this uncertainty by providing some theoretical constraints on the behavior of the pion form factor in the unphysical region, but none proved adequate.

Bebek et al. [16] embraced the use of theoretical input when they used the Born term model of Berends [12] to perform a form factor determination. Brauel et al. [17] similarly used the Born term model of Gutbrod and Kramer [18] to extract F_π. The presence of the nucleon and its structure complicates the theoretical model used, and so an unavoidable implication of this method is that the extraction of the pion form factor becomes model dependent.

Jefferson Lab E93-021 [19] similarly used the Regge model of Vanderhaeghen, Guidal, and Laget [13] to extract F_π. In this model, the pole-like propogators of Born term models are replaced with Regge propogators, and so the interaction is effectively described by the exchange of a family of particles with the same quantum numbers instead of the exchange of one particle. The model incorporates both the π ($J = 0$) and the ρ ($J = 1$) trajectories, with free parameters $\Lambda_{\pi,\rho}$, the π, ρ trajectory cutoff parameters, and fully takes into account off-shell effects without requiring a $g_{\pi NN}(t)$ factor. The Regge model does a superior job of describing the t dependence of the differential pion electroproduction cross sections of [17, 20] than the Born term model. Since the Regge model assumes a monopole form factor

$$F_\pi(Q^2) = [1 + Q^2/\Lambda_\pi^2]^{-1},$$

Λ_π is varied to obtain the best fit with the σ_L data, and F_π for that Q^2 found from substitution of Λ_π into the above equation.

Table 1: Description of old DESY and Cornell data. Pay particular attention to the large values of $|t|$ used for the large Q^2 measurements, and the poor attention to systematic errors.

Q^2 (GeV^2/c^2)	W (GeV)	$-t_{min}$ (GeV^2/c^2)	Reference	Comments
0.7	2.19	0.05	[17]	Full L/T separation and controlled systematics
1.2	3.11	0.019	[21]	High ϵ unseparated cross sections only. Hydrogen and π^-/π^+ data on deuterium data taken, and used for isoscalar correction to unseparated cross sections.
4.0	2.15	0.477	[21]	Same.
1.7	3.11	0.034	[21]	High ϵ unseparated cross sections only. Only hydrogen data taken. Isoscalar correction taken from π^-/π^+ measurements on deuterium at other kinematics.
2.0	2.15	0.157	[21]	Same.
1.2	2.15	0.069	[22]	High and low ϵ measurements obtained in different experiments, and combined for L/T separation later. Systematic error?
2.0	2.65	0.07	[22]	Same.
3.3	2.65	0.162	[22]	Same.
6.3	2.65	0.43	[23]	Only low ϵ data taken and t-channel Born Term model used to extract F_π. Uncontrolled systematic errors!
9.8	2.65	0.87	[23]	Same.

2.2 Older data and analyses

Unfortunately, the experimental knowledge of F_π is poor. Until 1978, the pion form factor in the space-like region was an active and mature field, after which time it went into dormancy due to the limitations of the existing electron accelerators. **The perception that F_π is difficult or impossible to extract at high Q^2 stems from the poor quality of these old data.** Table 1 summarizes the conditions under which they were obtained.

Table 1 shows that the situation above $Q^2 = 2.0$ GeV^2/c^2 degrades rapidly. For example, Bebek et al. [16] were unable to perform a L/T separation, and so were sensitive to the presence of isoscalar backgrounds. They were required to add an empirical isoscalar component to the theory of Berends before performing a F_π extraction, amounting to an approximately 10% correction. Where they were able to perform a L/T separation, the resulting uncertainties in σ_L were so large that for the actual determination of the pion form factor, σ_T was simply assumed to be proportional to the total photon cross section and subtracted from

Table 2: The ratio M_{pQCD}/M_{pole} from reference [24], using the King-Sachrajda nucleon distribution amplitude, as calculated for a number of high Q^2 results in Table 1.

Q^2 GeV^2/c^2	W GeV	$-t$ (GeV^2/c^2)	M_{pQCD}/M_{pole}
		0.01	0.18
1.94	2.67	0.07	0.12
3.33	2.63	0.17	0.18
6.30	2.66	0.43	0.81
9.77	2.63	0.87	2.82

the measured (differential) cross section to arrive at σ_L. Since no uncertainty was used in the assumed values of σ_T, the given uncertainties in their extracted values for F_π are (severely) underestimated. This, together with the already relatively large statistical and systematic uncertainties of those data, precludes a meaningful comparison with theoretical calculations, and led Carlson and Milana to conclude *"[we] question whether F_π has been truly determined for large Q^2"* [24].

In reference [24], Carlson and Milana point out that the existence of competing non-pole QCD processes complicate the extraction of F_π at large Q^2. This criticism stems from the large size of $|t|$ used in the Table 1 results, several of which have $-t_{min} > 20m_\pi^2$. The backgrounds calculated for a number of the above results are reproduced in Table 2. It is seen that the background ratio M_{pQCD}/M_{pole} rises dramatically once $-t_{min} > 0.20$. In order to avoid this problem *"more reliable measurements of F_π at high Q^2 require smaller $|t|$ and thus higher electron energy loss ν."* [24].

Our proposed measurements meet this requirement.

Table 3: Central arm kinematics used in E93-021. $W = 1.95$ GeV.

E_e (GeV)	θ_e (deg)	E_e (GeV)	θ_π (deg)	p_π (GeV/c)	Q^2 (GeV^2/c^2)	ϵ	$\lvert t\rvert$ (GeV^2/c^2)
2.445	38.40	.567	9.99	1.856	.60	.3749	.030
3.548	18.31	1.670	14.97	1.856	.60	.7369	.030
2.673	36.50	.715	11.46	1.929	.75	.4295	.044
3.548	21.01	1.590	15.45	1.929	.75	.7042	.044
2.673	47.26	.582	10.63	2.048	1.00	.3272	.071
3.548	25.41	1.457	15.65	2.048	1.00	.6469	.071
3.005	56.49	.594	10.49	2.326	1.60	.2722	.150
4.045	28.48	1.634	16.63	2.326	1.60	.6263	.150

2.3 E93-021 data and analysis

As an example of what is feasible, we present some results from the recently completed E93-021 experiment [19]. This experiment measured F_π with the HMS+SOS spectrometers in Hall C at the kinematics shown in Table 3. It can be seen that the $-t_{min}$ for central kinematics is kept below 0.15. Figure 3 shows the L and T separated cross sections from E93-021, plotted versus $-t$. This dependence on $-t$ was obtained by making full use of the acceptance of the spectrometers, and so differs slightly from the central ray kinematics listed in Table 3.

In parallel kinematics, it is not possible to hold W and Q^2 fixed, and still vary $-t$, since in this case they are not independent variables. In order to measure the dependence of σ_L versus $-t$, to test the success of the Regge model and aid in the extraction of F_π, θ_π was varied away from parallel kinematics. In this case, the LT and TT terms also contribute, and so additional data at $\pm 4^o$ from parallel kinematics were obtained at the high ϵ setting (where the pion arm was at sufficiently large angle to allow this). These response functions were obtained from the ϕ dependence of the data, and incorporated in the extraction of σ_L.

It is seen in figure 3 that that the Regge model predictions are in fair agreement with the σ_L data, but do not agree well with the σ_T data. However, since σ_L is dominated at small $|t|$ by the t-channel process, other processes should have only limited influence on the extraction of F_π from σ_L. This was checked in two ways. In the first, the ρ trajectory cutoff parameter, Λ_ρ, was varied and in the extreme case the ρ trajectory was omitted entirely. While this caused a large change in the prediction for σ_T, σ_L was nearly unaffected. In the second method, a background in σ_L, over and above the processes assumed in the Regge model, was added to the fit of the model prediction to the data. A number of different backgrounds were tried, and the variation in the value of F_π obtained was used to establish the model dependence of the result.

Figure 4 shows our preliminary results for F_π, and the boxed region near the bottom gives our estimate of the model dependence. While the new measurements have significantly smaller systematic errors than the old measurements, the two sets are consistent with each other. This lends confidence that this experimental method can be applied with success at even higher Q^2. It is also important to point out that because our experimentally measured $d\sigma_L/dt$ will be published in the literature, updated values of F_π could be extracted

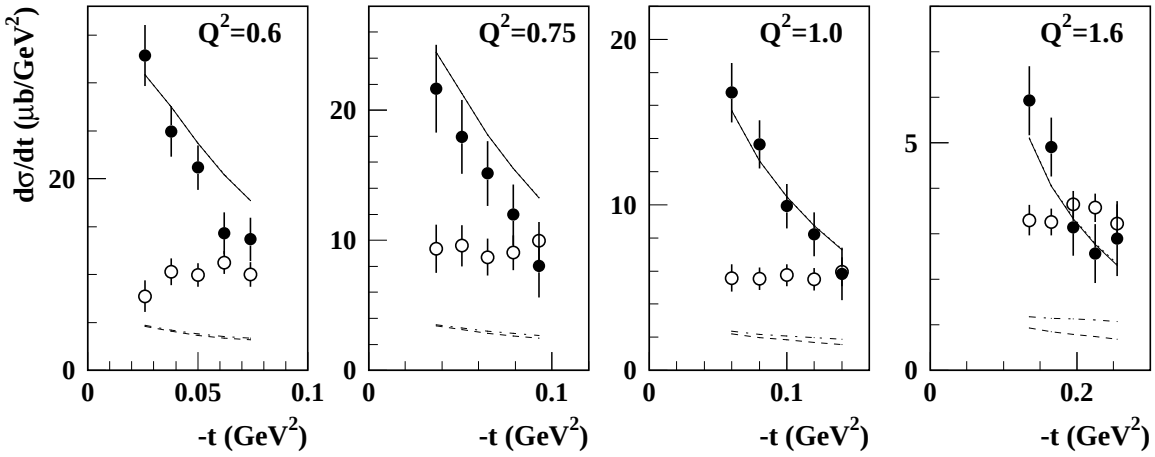

Figure 3: Separated cross sections from E93-021 [19]. The solid points are σ_L and the empty points are σ_T. The solid and dashed (dash-dotted) curves denote the predictions of the VGL Regge model [13] with cutoff parameters in the π and ρ trajectories of $\Lambda_\pi^2 = 0.4$ and $\Lambda_\rho = 0.6$ (2.1) GeV^2/c^2.

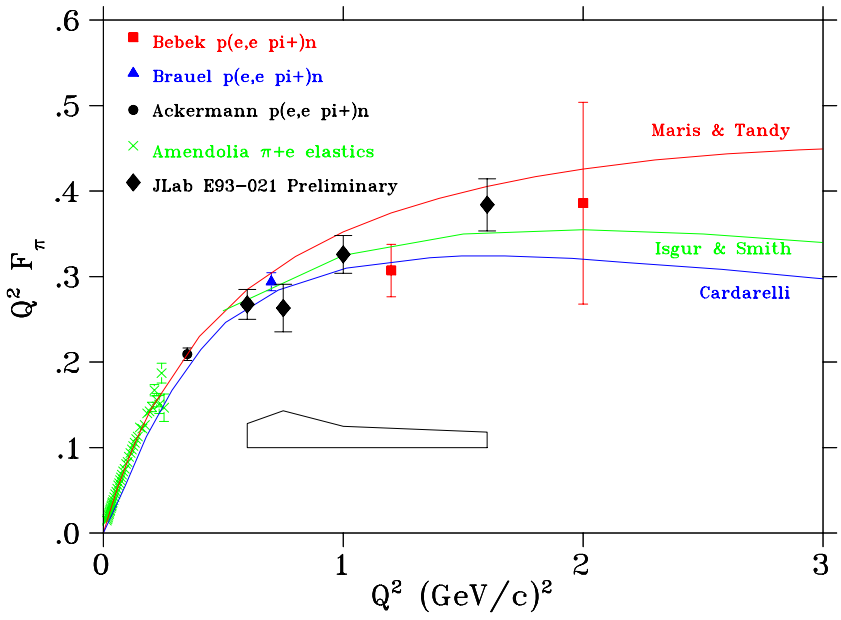

Figure 4: Preliminary F_π data from E93-021 [19], compared with the results from older experiments and theoretical calculations, as noted. The box near the bottom indicates the model sensitivity of the JLab result.

in the future, should even more sophisticated models for the $p(e,e'\pi^+)n$ reaction become available. The experimental result is not permanently 'locked in' to a specific model.

Given the success of E93-021, and the estimate of the non-pole background by Carlson and Milana [24], we are fully confident that we will be able to reliably able to extract $\mathbf{F_\pi}$ for $\mathbf{-t_{min}}$ up to 0.20 in the proposed 11 GeV upgrade experiment, as described below.

2.4 SHMS+HMS experiment at 11 GeV

2.4.1 Proposed kinematics

It is extremely important to note that the problems with the old high Q^2 data are not insurmountable. With few exceptions, they were taken with $W < 2.65$ GeV. The 11 GeV beam upgrade, and the good forward angle capability of the proposed SHMS, will allow data to be obtained at significantly higher W than before, which allows $-t_{min}$ to be placed significantly closer to the pole. In addition, backgrounds to the t-channel diagram in σ_L are expected to drop with increasing W, so the experiment should also be much cleaner and easier to interpret than the old measurements. A possible set of kinematics for this experiment are given in Table 4. They were chosen with the requirement that a L/T separation is performed with $\Delta\epsilon \approx 0.3$, which we have found to be the best compromise between good $\Delta\epsilon$ leverage, and a small $-t_{min}$.

Finally, we note that for the settings in Table 4, each spectrometer remains well below its maximum momentum setting. If the endstation maximum energy changes from 11 to 13.2 GeV (i.e., 20% higher) at constant luminosity, then the F_π program with HMS+SHMS will be able to benefit.

2.4.2 Simulation of the SHMS+HMS experiment

To obtain a better understanding of the experiment, we have modified the standard Hall C Monte Carlo package, SIMC, by replacing the SOS spectrometer with the proposed SHMS, and tracking $p(e,e'\pi^+)n$ coincidences through the SHMS+HMS combination. Simulated data distributions are presented for $Q^2 = 5$ GeV^2/c^2.

Figure 5 shows the kinematic overlap between the low and high ϵ settings of the spectrometers. To allow an excellent L/T separation to be obtained over a wide region of Q^2 and W, it will be necessary to take two low ϵ settings for each Q^2, at slightly different W.

As mentioned earlier, it is not possible to hold W and Q^2 fixed in parallel kinematics, and still vary $-t$. In order to measure σ_L data versus $-t$, it is necessary to obtain data for $\theta_{\pi q} \neq 0$, where LT and TT also contribute. Figure 6 shows simulated SHMS+HMS data where θ_{SHMS} is varied by $\pm 2^o$ from the parallel kinematic position. The excellent ϕ coverage allows LT and TT to be obtained in an efficient manner.

Table 4: Parallel kinematics for proposed $p(e,e\pi^+)n$ measurement in Hall C with HMS+SHMS and 11 GeV maximum beam energy. Additional runs at other kinematics are also required, as described in the text. The event rates assume 50 μA beam on 8 cm target.

E_e	E_e	θ_e	ϵ	$\|t\|$	p_π	θ_π	η_π	$d^3\sigma/d^2\Omega dE$	Time
GeV	GeV	deg		GeV^2/c^2	GeV/c	deg		pb/sr^2MeV	$hr/10^4Events$
$Q^2 = 1.00GeV^2/c^2, W = 3.00GeV$									
6.000	1.140	22.036	0.349	0.012	4.850	-4.948	0.929	0.87	12.0
7.000	2.140	14.842	0.545	0.012	4.850	-6.345	0.929	2.73	2.4
7.600	2.740	12.579	0.626	0.012	4.850	-6.909	0.929	4.36	0.8
$Q^2 = 2.00GeV^2/c^2, W = 3.40GeV$									
8.300	1.543	22.787	0.341	0.026	6.740	-4.968	0.948	0.85	8.7
9.000	2.243	18.107	0.452	0.026	6.740	-5.797	0.948	1.55	3.2
10.000	3.243	14.264	0.573	0.026	6.740	-6.648	0.948	2.92	1.6
10.600	3.843	12.720	0.628	0.026	6.740	-7.042	0.948	3.95	0.4
$Q^2 = 3.00GeV^2/c^2, W = 3.40GeV$									
8.600	1.310	29.896	0.273	0.054	7.258	-5.002	0.952	0.67	6.6
9.000	1.710	25.501	0.343	0.054	7.258	-5.641	0.952	0.99	3.4
10.000	2.710	19.149	0.484	0.054	7.258	-6.816	0.952	2.05	1.1
11.000	3.710	15.581	0.588	0.054	7.258	-7.644	0.952	3.47	0.5
$Q^2 = 4.00GeV^2/c^2, W = 3.30GeV$									
8.600	1.134	37.337	0.227	0.098	7.411	-5.109	0.953	0.58	8.7
9.000	1.534	31.216	0.300	0.098	7.411	-5.907	0.953	0.88	4.3
10.000	2.534	22.912	0.449	0.098	7.411	-7.336	0.953	1.86	1.2
11.000	3.534	18.456	0.559	0.098	7.411	-8.325	0.953	3.18	0.5
$Q^2 = 5.00GeV^2/c^2, W = 3.30GeV$									
9.100	1.101	41.349	0.203	0.142	7.920	-5.029	0.956	0.44	11.8
10.000	2.001	28.940	0.352	0.142	7.920	-6.698	0.956	0.99	2.9
11.000	3.001	22.438	0.480	0.142	7.920	-7.930	0.956	1.82	1.1
$Q^2 = 6.00GeV^2/c^2, W = 3.20GeV$									
9.200	1.015	47.244	0.177	0.212	8.070	-5.006	0.957	0.33	16.2
10.000	1.815	33.409	0.313	0.212	8.070	-6.719	0.957	0.72	4.4
11.000	2.815	25.427	0.447	0.212	8.070	-8.134	0.957	1.35	1.5

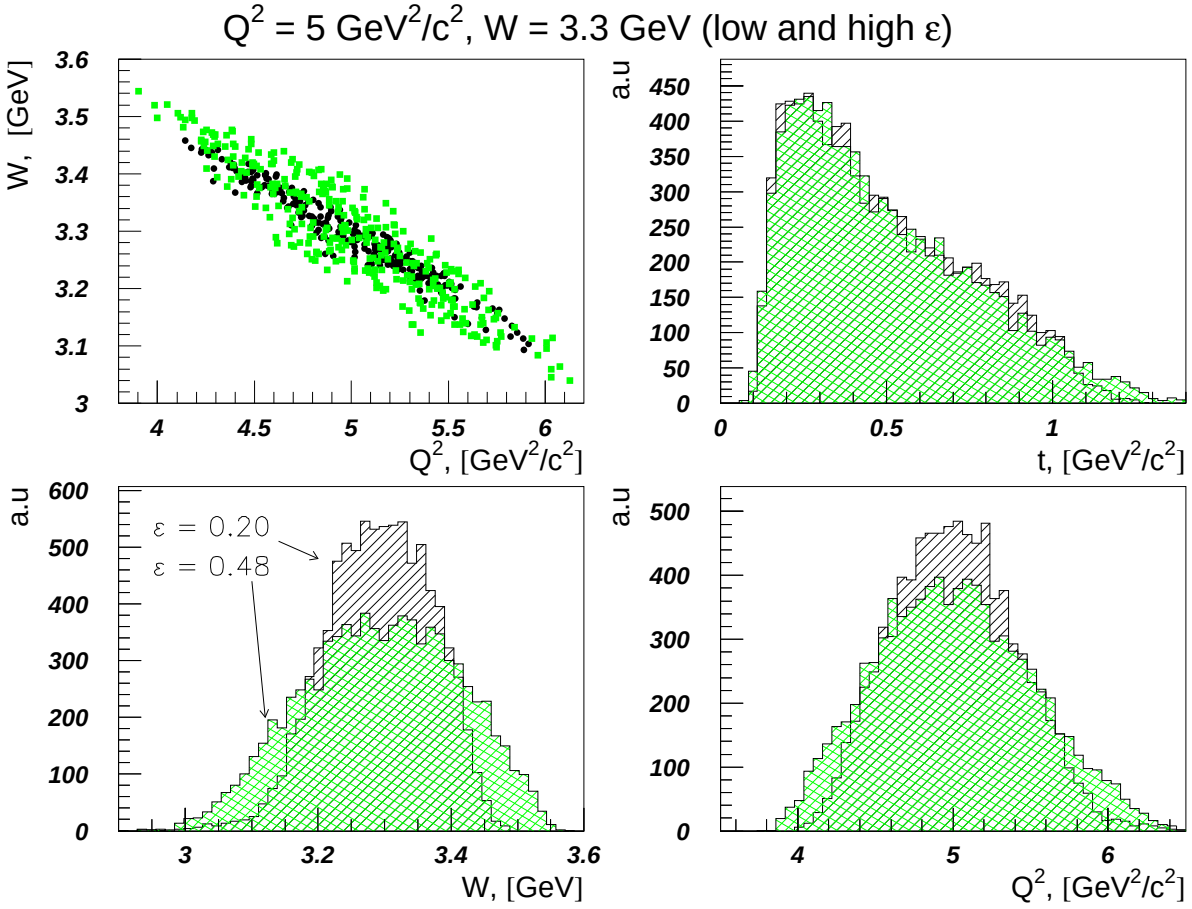

Figure 5: $Q^2 = 5$ simulated distributions in the SHMS+HMS spectrometers. The green points are the high ϵ setting, as listed in table 4. The black points are the low ϵ setting, with $\theta_{SHMS} = 5.5^o$.

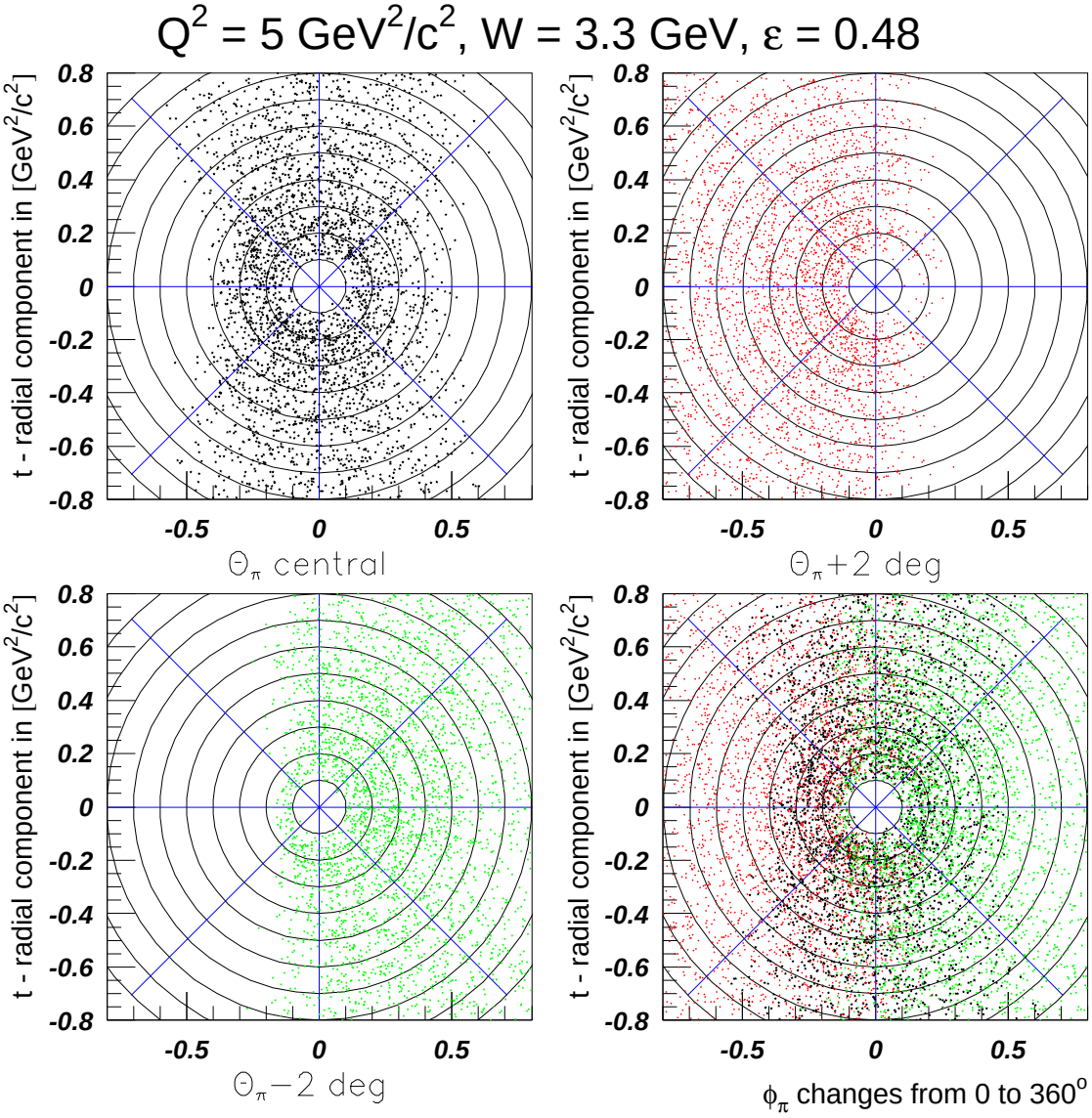

Figure 6: ϕ versus $-t$ coverage for settings as labelled. The figures are polar plots, with $-t$ as the radius, and ϕ as the angle. 2π coverage in the lower right panel indicates the $-t$ range available for LT and TT extraction. Cuts were placed to match W-Q^2 range of the low ϵ setting in Figure 5.

2.4.3 Particle identification and expected rates

The HMS will be configured for e^- detection in this experiment, using the standard combination of a gas Čerenkov (about .75 atm C_4F_{10}) and lead glass calorimeter. e^- and π^- singles rates were computed using Reference [25], and are listed in Table 5. We see that the π^-/e^- ratio is generally in the (several 100):1 range, so we anticipate that no problems will arise that weren't already successfully resolved in our completed E93-021 measurement.

The SHMS will be used for π^+ detection, and will sit at very forward angles. Expected singles and accidental coincidence rates are listed in Table 5. In all cases, we see that they are well below the maximum rate capabilities of the focal plane instrumentation. At higher momenta, particle identification becomes qualitatively more difficult because one can no longer separate pions and protons by TOF. The 1 meter long high pressure gas Čerenkov (1 atm C_4F_{10}) will be used to separate pions from heavier particles. With this particular gas fill, kaons will not cross cerenkov threshold until about 9 GeV/c, which is well above the maximum pion momentum settings. Positrons would be identified by a lead-glass calorimeter. Since the there should not be many positrons with $> 80\%$ of the beam momentum, a supplemental Čerenkov should not be necessary.

In total, we believe that the requirements of the F_π experiment are compatible with the proposed SHMS instrumentation and acquisition systems.

Table 5: Projected singles and accidental coincidence rates assuming 50 μA beam on 8 cm Hydrogen target. The coincidence rate assumes a resolving time of 40 ns, and a detector efficiency of 0.8.

ϵ	HMS e^- rates Hz	HMS π^- rates Hz	SHMS π^+ rates Hz	SHMS Proton rates Hz	Random coinc. $e^- \cdot (\pi^+ + \mathrm{p})$ Hz	Real coinc. $e^- \cdot \pi^+$ Hz
$Q^2 = 1.00 GeV^2/c^2, W = 3.00 GeV$						
0.349	2100	380000	15500	4160	0.8	0.2
0.545	9560	225000	24700	6160	5.8	1.2
0.626	17900	175000	26200	6800	11.8	8.9
$Q^2 = 2.00 GeV^2/c^2, W = 3.40 GeV$						
0.341	1100	192000	6000	1920	0.2	0.3
0.452	2650	121000	11050	2540	0.8	1.2
0.573	6500	71800	16100	2540	2.4	1.7
0.628	10000	56000	8400	2540	2.2	6.9
$Q^2 = 3.00 GeV^2/c^2, W = 3.40 GeV$						
0.273	320	123800	3160	1200	0.02	0.4
0.343	582	83600	4390	1500	0.06	1.2
0.484	1700	38900	3575	1300	0.16	2.6
0.588	3700	22000	3110	1140	0.4	6.2
$Q^2 = 4.00 GeV^2/c^2, W = 3.30 GeV$						
0.227	120	84800	2260	950	0.008	0.3
0.300	230	50150	2630	1030	0.02	0.7
0.449	740	18700	1785	750	0.04	2.3
0.559	1650	9200	1370	590	0.06	5.6
$Q^2 = 5.00 GeV^2/c^2, W = 3.30 GeV$						
0.203	60	63500	1485	690	0.002	0.2
0.352	240	18400	1330	600	0.008	1.0
0.480	600	7200	870	400	0.02	2.6
$Q^2 = 6.00 GeV^2/c^2, W = 3.20 GeV$						
0.177	25	50000	1200	600	0.001	0.2
0.313	90	13000	960	465	0.002	0.6
0.447	245	4165	545	275	0.004	1.9

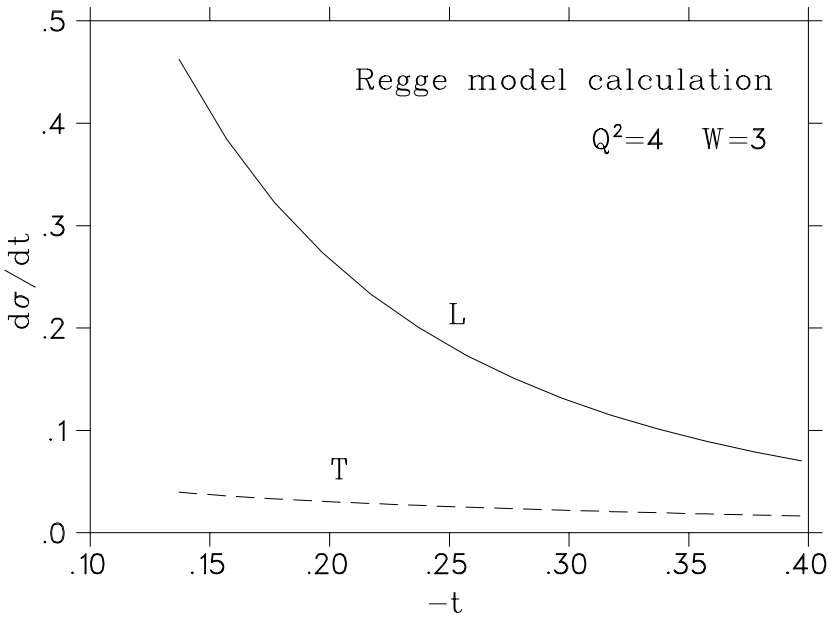

Figure 7: Regge model [13] calculation of the L and T responses in the $p(e,e'\pi^+)n$ reaction. The π trajectory cutoff value used is consistent with the E93-021 σ_L data. The curves terminate at $-t_{min} = 0.138$, corresponding to parallel kinematics.

2.4.4 Projected error bars and beam time estimate

We have modelled the expected cross sections, based on the E93-021 and low Q^2 Cornell results, and cross checked with the σ_L predictions of the Regge model (Figure 7). Expected $(e,e'\pi^+)$ coincidence rates, assuming 50 μA beam and 8 cm target, are listed in the right column of Table 5.

Assuming uncorrelated errors between the high and low ϵ measurements, the experimental error in F_π is

$$\frac{\Delta F_\pi}{F_\pi} = \frac{1}{2}\frac{1}{(\epsilon_1-\epsilon_2)}\frac{\Delta\sigma}{\sigma}\sqrt{(R+\epsilon_1)^2+(R+\epsilon_2)^2}.$$

As far as the extraction of the form factor is concerned, the relevant quantities are $R = \sigma_T/\sigma_L$ and $\Delta\epsilon$ between the two kinematic settings.

The T/L ratios assumed here are listed in Table 6, and the corresponding projected error bars (assuming 1% statistical and 3% systematic error) for the experiment are listed in Table 6 and displayed in Figure 8. As the assumed T/L ratios are more pessimistic than indicated by the Regge model calculation (Figure 7), these error bars are realistically achievable by the experiment. We see that the new measurement is easily able to distinguish between at least a number of the models, as shown in Figure 8.

A thoroughly designed experiment, designed to obtain sufficient data to constrain the t-channel model and obtain F_π in a systematic manner would include the multiple ϵ settings for each Q^2 listed in Table 4, and in addition, for each setting, would take data for:

1. $p(e,e'\pi^+)n$ at parallel kinematics for F_π extraction, as listed in Table 4. At low ϵ, this would entail the acquisition of two slightly different W settings, to match the W, Q^2 acceptance of the high ϵ setting.

Table 6: Expected errors for F_π assuming statistical error of 1% and systematic error of 3%. Model errors are not included.

Q^2	W	Systematic	Statistical	σ_T/σ_L	$\Delta\epsilon$	$\Delta F_\pi/F_\pi$
$(GeV/c)^2$	GeV	%	%			%
1.0	3.0	3	1	0.11	0.28	5.0
2.0	3.4	3	1	0.48	0.29	7.6
3.0	3.4	3	1	0.5	0.32	6.6
4.0	3.3	3	1	0.6	0.33	6.8
5.0	3.3	3	1	0.7	0.28	8.4
6.0	3.2	3	1	0.8	0.27	9.3

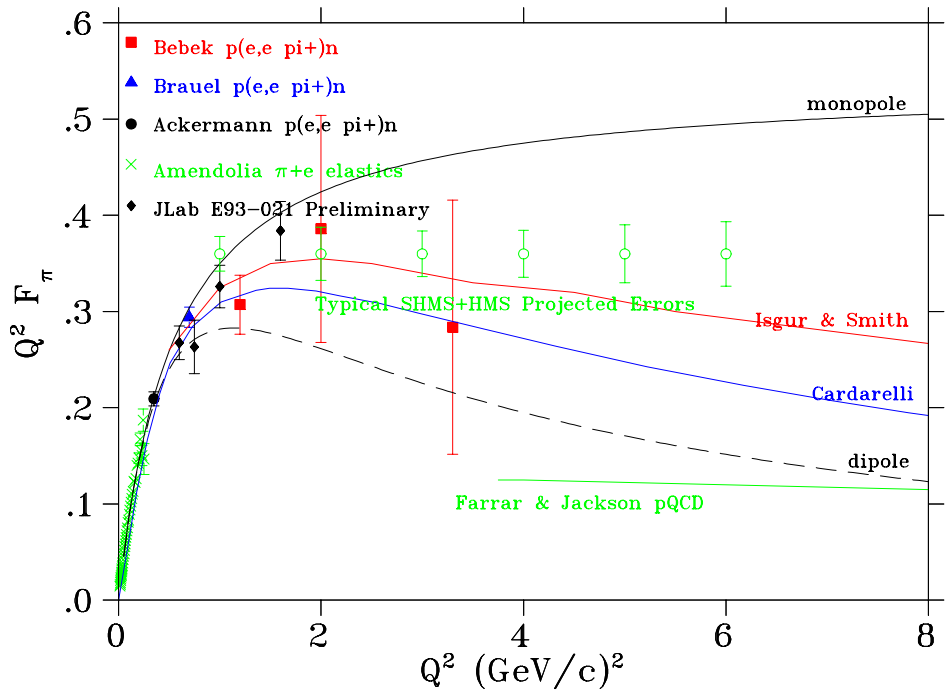

Figure 8: Projected error bars for the SHMS+HMS experiment, in comparison with a variety of theoretical models, and existing data.

2. Extra $p(e,e'\pi^+)n$ data at $\pm 2^o$ away from parallel kinematics at the high ϵ setting to determine LT, TT.

3. $d(e,e'\pi^\pm)$ on deuterium target, to measure the π^-/π^+ ratio, and test the t-channel dependence of the σ_L data.

Assuming 50 μA beam current incident on 8 cm target, and 70% detector and acquisition efficiency, we estimate that the entire experiment could be completed with 40 days of beam.

3 Summary

The high quality, continuous electron beam of Jefferson Lab makes it the only place to seriously pursue a program of F_π measurements. In 1997, E93-021 obtained data up to $Q^2 = 1.6$ GeV^2/c^2 in Hall C, and we expect to extend these measurements to $Q^2 = 2.6$ GeV^2/c^2 in 2002. However, a challenge of the QCD-based models in the most rigorous manner requires the electron beam upgrade and construction of the SHMS. An 11 GeV beam energy will allow measurements to be obtained sufficiently close to the π^+ pole that σ_L will be dominated by the t-channel process, and that backgrounds to σ_L will be minimized. The requirements upon the spectrometer are small forward angle capability, good angular reproducibility (to control systematic errors in the L/T separation) and sufficient missing mass resolution to cleanly separate $p(e,e'\pi^+)n$ events from $p(e,e'\pi^+)n\pi^0$. This combination will allow F_π to be determined in the best manner allowable by current models, and would provide a very significant advance in the understanding of the pion form factor.

Acknowledgements

We would like to thank A. Kozlov, S. Li, and J. Volmer for their considerable assistance with the calculations presented in this document.

References

[1] G.R. Farrar, D.R. Jackson, Phys. Rev. Lett. **43** (1979) 246.

[2] N. Isgur, C.H.L. Smith, Phys. Rev. Lett. **52** (1984) 1080.

[3] O.C. Jacob, L.S. Kisslinger, Phys. Lett. **243B** (1990) 323.

[4] R. Jakob, P. Kroll, Phys. Lett. **315B** (1993) 463.

[5] C.R. Munz et al., Phys. Rev. C **52** (1995) 2110.

[6] J.F Donoghue, E.S. Na, Phys. Rev. D **56** (1997) 7073.

[7] V.M. Braun, A. Khodjamirian, M. Maul, Phys. Rev. D **61** (2000) 073004.

[8] P.C. Tiemeijer, J.A. Tjon, Phys. Lett. **277B** (1992) 38.

[9] H. Ito, W.W. Buck, F. Gross, Phys. Lett. **287B** (1992) 23.

[10] P. Maris, P.C. Tandy, nucl-th/0005015.

[11] F. Cardarelli et al., Phys. Lett. **332B** (1994) 1.
F. Cardarelli et al., Phys. Lett. **357B** (1995) 267.

[12] F.A. Berends, Phys. Rev. D **1** (1970) 2590.

[13] M. Vanderhaeghen, M. Guidal, J.-M. Laget, Phys. Rev. C **57** (1997) 1454.
M. Vanderhaeghen, M. Guidal, J.-M. Laget, Nucl. Phys. **A627** (1997) 645.

[14] W.R. Frazer, Phys. Rev. **115** (1959) 1763.

[15] B.H. Kellett, C. Verzegnassi, Nuo. Cim. **20A** (1974) 194.

[16] C.J. Bebek et al., Phys. Rev. D **9** (1974) 1229.

[17] P. Brauel et al., Z. Phys. C **3** (1979) 101.

[18] F. Gutbrod, G. Kramer, Nucl. Phys. **B49** (1972) 461.

[19] J. Volmer, Ph.D. thesis, Free University of Amsterdam, 2000.
J. Volmer et al., Phys. Rev. Lett., in preparation.

[20] H. Ackerman et al., Nucl. Phys. **B137** (1978) 294.

[21] C.J. Bebek et al., Phys. Rev. D **13** (1976) 25.

[22] C.J. Bebek et al., Phys. Rev. Lett. **37** (1976) 1326.

[23] C.J. Bebek et al., Phys. Rev. D **17** (1978) 1693.

[24] C.E. Carlson, J. Milana, Phys. Rev. Lett. **65** (1990) 1717.

[25] Electron rate: Program QFS , J.W. Lightbody and J.S. O'Connell.
Hadron rates: Program EPC, J.S. O'Connell and J.W. Lightbody.